# An Experimental Study of Thermal Performance of an Organic Two-Phase Closed Thermosyphon in Waste Heat Extraction

دراسة عملية لأداء سيفون حرارى عضوي ذي طورين في إستخلاص الحرارة المفقودة

M.A. Elmougith, A.A. Hegazi, M.M. Awad and G.I. Sultan

*الملخص العربي:-* يُعتبر السيفون الحراري المغلق هو أحد أهم تطبيقات إنتقال الحرارة نظراً لعدم إحتياجه لطاقة ميكانيكية أو كهربية لتشغيلة. في هذه التجربة تم إستخدام سيفون حراري بقطر داخلي 1.8 سم وقطر خارجي 2.5 سم وطول 100 سم بحيث يكون طول المبخر والمكثف 40 سم كلاهما، وتمت تجربة بعض الموائع العضوية مثل (البنزين ، اثير البترول ، الأسيتون ، محلول الأسيتون ، والكلوروفورم) بحجوم مختلفة مثل 25%، 50% و 100% من حجم المبخر. تم إختبار اداء السيفون الحراري العضوي في إستعادة الحرارة المفقودة الناتجة من عملية إحتراق الوقود داخل محرك الديزل في صورة عادم قبل خروجه للجو. النتائج أثبتت أن السيفون الحراري العضوي يمكن إستخدامه لعمليات إستعادة الحرارة المفقودة ذات الجودة أو درجة الحرارة المنخفضة ، وأعلى قدرة للسيفون الحراري سُجلت عند إستخدام البنزين بحجم 50% من حجم المبخر، ايضاً النتائج اثبتت انه عند تركيب المبادل الحراري، قل تركيز أول أكسيد الكربون من العادم إلى نحو 19.33% عند استخدام البنزين كمائع تشغيل بحجم 50% من المبخر وعند سرعة دوران للمحرك 2700 لفة بالدقيقة.

*Abstract* – **Thermosyphon and passive heat exchanging devices become more popular in industrial applications due to its high capability of transferring heat with low fabrication cost. In this experiment, a thermosyphon made of copper with an internal diameter of 1.8 cm and outside diameter of 2.5 cm was investigated in recovering the wasted heat from a 4-stroke, 4-cylinder diesel engine. Waste heat from the engine comes in form of exhaust which is emitted to the atmosphere at higher temperatures. The evaporator section, which is 40 cm in length, is attached to a duct which has internal fins to guide the exhaust to take a certain path before being emitted into the atmosphere. The evaporator section was filled with various organic working fluids such as acetone, water-acetone mixture, benzene, chloroform, and petroleum ether at various filling ratios (FR) of 25%, 50%, and 100%. The condenser section was 40 cm in length, while the coolant was water passing through a cooling jacket attached to the condenser at various mass flow rates from 1 to 5 gm/sec. The experiment was taken place under three different heat input or engine speeds at 1400, 2100 and 2700 rpm. The best thermal performance of the thermosyphon results when being charged with a filling ratio FR= 50%, this agreed much with the literature reviews even when using an organic working fluid, besides, FR=25% comes in the second place and FR= 100% was the worst. Benzene ($C_6H_6$) showed great thermal performance over the others, acetone ($C_3H_6O$) comes in the second place, while the worst working fluid among others was petroleum ether ($HC_3$-O-$CH_3$). It was also found that heat exchanging process resulted in a sensible reduction of CO concentration. The maximum average reduction percentage of CO was found to be 19.33% at FR=50% benzene at engine rotational speed of 2700 rpm.**

*Prof. Dr. G. I. Sultan, Mechanical Power department, Faculty of Engineering, Mansoura University (gisultan@mans.edu.eg)*

*Prof. Dr. M. M. Awad, Mechanical Power department, Faculty of Engineering, Mansoura University (m_m_awad@mans.edu.eg)*

*Dr. A. A. Hegazi, Mechanical Power department, Faculty of Engineering, Mansoura University (ahmedabd_elsallam@yahoo.com)*

*M. A. Elmougith, Mechanical Power department, Faculty of Engineering, Mansoura University (Mohamed.abdo@students.mans.edu.eg).*

## NOMENCLATURE

| | |
|---|---|
| A | tube surface area (m$^2$) |
| C | Zuber constant |
| $C_f$ | flow coefficient |
| $C_p$ | specific heat (kJ/kg.K) |
| $D_o$ | outside diameter of the tube (m) |
| $D_i$ | inside diameter of the tube (m) |
| g | gravitational acceleration (m$^2$/sec) |
| h | specific enthalpy (kJ/kg) |
| H | height (m) |
| L | length of the tube (m) |
| $\dot{m}$ | mass flow rate (kg/sec) |
| Pr | Prandlt number |
| $\bar{\bar{q}}$ | heat flux (W/m$^2$) |
| T | temperature (K) |
| U | overall heat transfer coefficient (W/m$^2$.K) |
| v | volume (m$^3$) |
| V | velocity (m/sec) |

### GREEK LETTERS

| | |
|---|---|
| μ | dynamic viscosity (kg/m.s) |
| ρ | density (kg/m$^3$) |
| σ | surface tension (N/m) |

### SUBSCRIPTS

| | |
|---|---|
| f | liquid |
| $i$ | inlet condition |
| m | mean |
| o | outlet condition |
| $v$ | vapor |

### ABBREVIATIONS

| | |
|---|---|
| cr | critical |
| con | condenser |
| eqv | equivalent |
| evp | evaporator |
| exh | exhaust |
| FR | filling ratio |
| HEx | heat exchanger |
| min | minimum |

## I.   INTRODUCTION AND LITERATURE REVIEWS

In the presence of increasing power consumption globally, high emitted pollutants and low thermodynamic efficiencies, scientists put their effort to improve the efficiencies and make the best use of energy. The Kelvin-Planck statement – which is also known as the 1st form - of the second law of thermodynamics, refers that, there is no ideal heat engine as it is impossible to convert all the heat from a hot reservoir into a useful work, there would be for sure some amount of heat transferred or exhausted to a cold reservoir[1]. As a result, there is no 100% thermally efficient heat engine. On the other hand, the maximum theoretical efficiency of any heat engine is the Carnot efficiency. In the

perspective of statistics, consumption of oil, as an energy source in 1998 to 2016 has dramatically increased to reach 13,276 million metric tons in 2016 which is about 47% more in the usage of the fossil resources [2].This lead engineers and scientific society to find out a thermally effective, cost-effective and alter industrial applicable solutions for heat recovery processes[3]. Waste heat recovery technologies are varied and there are many types of heat exchanging devices which are doing what they aimed for. The passive heat exchanger is one of the most economical solutions that could be applicable in industrial processes because of its ability to transfer a large amount of heat without needing a power source, electricity or fuel consumption. Many studies have done, and are going to be, in passive heat exchanging, the most known two main devices of passive heat transfer are the thermosyphon and heat pipes. Thermosyphon depends on the density difference of the working fluid phases (liquid and gas) and the driving force is the gravity, as a result, the evaporator section of the thermosyphon should be below the condenser section. Heat pipes work with the same phenomena, but the driving force is the capillary action, as a result, it could work horizontally. Thermosyphon consisted of three main sections: an evaporator section, an adiabatic section and a condenser section as shown in Fig.1
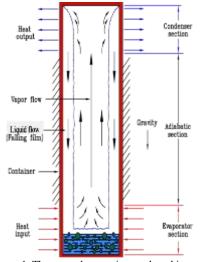


Figure 1. Thermosyphon sections and working principle

The evaporator contains the working fluid at a certain filling ratio where the working fluid begins to evaporate under the rules and correlations of pool boiling phenomena, the vapor then rises to the condenser section, where it gives off its latent heat, to be condensed again to the evaporator section in a closed repeated cycle inside the tube[4]. Many considerable researches were conducted on the thermal performance of the thermosyphon within different theoretical and experimental parameters [5-12]. Shiraishi et al., [6] tested experimentally a -37 mm diameter, and 4 mm thickness – copper tube divided into three main sections, 280 mm evaporator section, 500 mm adiabatic section, and 450 mm condenser section with three working fluids; water, ethanol and R113 at different filling ratios. They committed that the overall thermal resistance has a potential relationship with the filling ratio, then they developed a mathematical model to predict the thermal

performance at different experimental parameters. Terdtoon et al., [8] investigated the influence of aspect ratio (Le/d), and Bond number (Bo) using three thermosyphon made of copper. The variable of their experiment was the aspect ratio and the inclination angle, and the normal position at 90o. They concluded that there is a correlation between aspect ratio and the inclination angle of the thermosyphon. They found that the ratio of the highest heat transfer rate of the inclined thermosyphon to that the normally positioned (vertical) one decreased within Le/d < 10, and remained constant at Le/d > 10, while Bond number had nothing to do with the inclination angle when the highest heat transfer occurred. Imura et al., [5] studied experimentally the effect of several parameters, such as the evaporator length, working fluid, filling ratio and tube diameter on the critical heat flux. The working fluids were water, ethanol, and R113. They correlated their data as the following:

$$q_{cr} = 0.64 h_{fg} \left(\frac{\rho_i}{\rho_v}\right)^{0.13} \left(\frac{d_i}{4L_e}\right) [g\sigma\rho_v{}^2(\rho_i - \rho_v)]^{0.25} \quad ..(1)$$

Negishi and Sawada [7] also investigated the effect of inclination angle and filling ratios on the thermal performance of the thermosyphon. They tested water and ethanol as working fluids. They found that there is a necessity to work under filling ratio within range 25 to 60% while water was the working fluid, while 40 to 70% while ethanol was the working fluid, in addition, the optimum performance observed while the inclination angle was between 200 and 400 for water and more than 50 for ethanol. Shalaby et al., [9] tested a smooth copper tube of length 1500 mm, evaporator length was 600 mm, condenser length was 600 mm, and an adiabatic length of 300 mm. Their results coherent the optimum filling ratio to be 50% of the evaporator volume, while the maximum thermal performance was obtained at a 30° inclination angle. Park et al., [10] investigated the effect of the filling ratio on the overall heat transfer coefficient of both the evaporator and condenser sections on a copper container filled with FC-72. Their experiment heat input range was within 50 – 600, and FR within 10 – 70%. They concluded that the filling ratio has a neglected effect on the heat transfer coefficient of the evaporator section, while as the filling ratio increases, the heat transfer coefficient of the condenser significantly increases. Ziapour and Shaker,[11] developed a Fortran code to predict the thermal resistance effects on the heat transfer characteristics using different refrigerants such as water, ammonia, R-11, R-22, and R-134a. Their results showed great agreement with experimental results conducted by other research. Naresh and Balaji, [12] tested an internally finned type. The tested filling ratio ranged between 20 to 80% for water and acetone. Their experiment heat input range was 50 – 275 W. They also concluded that the optimum performance was observed when using a filling ratio of 50%, in addition, installing fins at the condenser enhanced the thermal performance by 35.48% at low loads. Some other considerable researches were conducted to investigate the applicability of the passive heat devices into an industrial approaches [13-17]. Baghban and Majideian [14] investigated an air-air heat pipe heat exchanger at a temperature range of 15 – 55 ℃ in hospital and laboratories, where the air needs to be changed for 40 times in an hour. Heat pipes were filled with acetone, water,

and methanol. Their results showed a great agreement with the mathematical model. The low efficiency of their results was a cause of high pitch to diameter ratio, and when a small number of heat pipes were attached. Chen and Yang, [16] investigated the influence of using loop thermosyphon in cooling high concentrator photovoltaic cells (HCPV)  by simulating a photovoltaic cell with a 156 cm wide and implemented five independent loop thermosyphon. The condenser was a spiral-finned tube made of carbon steel. The outside diameter of the base tube was 25 mm with a 1 mm thickness. They found that the rate of heat transfer by acetone was 199.5 Watts, which was 1.97 times that of ethanol and 5.49 times that of water. Another deduced hypothesis was that the total heat dissipation was reduced by 37.93% when they increased the fin spacing from 5mm to 15mm. Orr et al., [17] investigated a conjunction system of thermoelectric generators (TEGs) and heat pipes. They experimentally investigate the combination of these two devices. They used thermoelectric generators to make use of temperature differences with the help of the Seebeck effect. The temperature variance between the two substances produces a voltage difference between the two substances although the produced voltage by the Seebeck effect. Wadowski et al., [13] investigated hysteresis in gas-to-gas thermosyphon based heat exchangers for low-temperature difference heat recovery applications, and the effect of the implementation of a trigging system on the heat exchanger performance and the advantages of this system in commercial applications. Their thermosyphon heat exchanger unit consisted of three rows of pipes each had six inline pipes separated by 36 mm, the pipes cover was a rectangular shape of 99.3 mm width and 305 mm length. Thermosyphon tubes are made of copper with an ID of 15.5 mm and OD of 16.4 mm each was charged with 50 g of R-22 refrigerant. They recorded the influences of the trigger system as the first test they turned on the heaters at the sixth minute and turned it off at the eighth minute, as a result, the evaporator section recorded a peak temperature of $39^0$ C and then returned to its original temperature. While the effectiveness reached 38% instead of the initial past value of 16%, then it dropped to 30% and standstill until the end of their experiment.

In our experiment, we investigated experimentally the thermal performance of the thermosyphon in low waste heat recovery applications. The waste heat source was considered as a 4-stroke, 4-cylinders, water cooled diesel engine, while the tested organic fluids were; acetone, water-acetone, petroleum ether, benzene and chloroform at different filling ratios of 25, 50 and 100% and different engine speeds of 1400, 2100 and 2700 rpm. Some considerable reviews were found in the field of pollutants and its control, Considerable experiments and researches were conducted to measure the pollutants concentration and its effects on health and the environment and also the heat recovery technologies and its effects on the concentration of pollutants [18-23]. Prasad and Bella, [21] mentioned that the typical composition and concentration of diesel exhaust emissions are (100 – 10000 ppm) for CO, (50 – 500 ppm) for HC, (30 – 1000 ppm) for NOx, (20 – 200 mg/m$^3$) for diesel particulate matters (DPM), and (2 – 12 vol %) for $CO_2$ concentration. Hamdeh, [18] treated the exhaust gas internally by studying the effect of

cooling the recirculated exhaust gases (EGR) on diesel emissions and pollutants concentration using spiral fin pipes as a heat exchanger that cooled the recirculated exhaust gas temperature before mixing with the intake charge, as a result, he found that the intake charge temperature was decreased which led to poor combustion and increased the carbon monoxide (CO) concentration. Ning et al., [19] investigated experimentally the effect of cooling the exhaust gas on diesel particulate. As cooling the exhaust temperature can result in condensation of volatile materials and coagulation of particulates; they used a water cooler to adjust the exhaust. They concluded that the main reason for increasing the mass concentration while cooling the exhaust gas is that the volatile organic/inorganic substances were nucleated or condensed during the cooling process and results in decreasing other gaseous emissions. Charalampos et al.,[22] studied the effect of cooling the exhaust temperature on gas exhaust emissions by passing the exhaust through a radiator with an attached front axial fan to cool down the exhaust temperature for different fuels. They concluded that CO and $CO_2$ sensibly decreased after attaching the radiator. The aim of this study is to figure out the thermal performance of the two-phase closed thermosyphon in low waste heat recovery applications using suitable organic working fluids and studying the influences of the heat exchanging process on the carbon monoxide concentration.

inlet and outlet points of the exhaust duct (13) to measure the temperature of the exhaust before and after passing the heat exchanger.
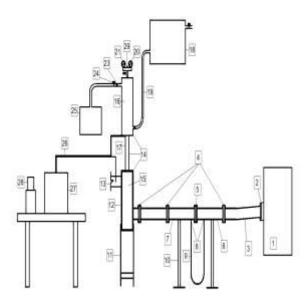


Figure 2. Experiment test rig layout

## II.   EXPERIMENTAL PROCEDURES

In order to investigate the thermal performance of the thermosyphon in low waste heat recovery applications, we considered the diesel engine as a waste heat resource, which emits exhaust into the atmosphere at high temperatures. Fig.2 shows the layout of the experiment which consists of three main parts; the diesel engine (1), the exhaust duct (12) and the thermosyphon (15, 16 and 17). The exhaust duct was attached to the engine exhaust manifold throughout carbon steel pipes (3 & 6) and connecting flanges (2 & 4). The carbon pipes, the duct and the thermosyphon sections were insulated using glass wool (14) to minimize the heat transferred to the surroundings. An orifice plate (5), with a bore diameter of 2.5 cm and a diameter of 5 cm, was installed in the middle of the carbon steel pipe with two welded pressure tapings (8) placed in one diameter upstream and half a pipe diameter downstream. To measure the flow rate of the exhaust through the pressure head differences across the manometer tube (9) throughout the manometer fluid (25), which is glycerol.

The evaporator section was placed into the duct penetrating a three internally welded baffles, while a cooling jacket (16) was attached to the condenser section to let the cooling water exchange heat with the condenser. Two pressure gauges (20 & 21) were attached to measure the vacuum and operating pressure of the thermosyphon. 6 pre-calibrated thermocouples (26) were attached in 10, 20, 30, 40, 50 and 60 cm from the bottom of the evaporator to measure the temperature distribution along the thermosyphon tube, and two digital thermocouples were attached at the inlet and outlet points of the condenser to measure the temperature of the cooling water. Two thermocouples were attached also at the

All thermocouples were connected to a YOKOGAWA 24 channels temperature recorder (27), which was set up to determine the temperature readings at each point. A make-up water float valve tank (18) was attached in 3 meter above the ground to ensure a steadily mass flow rate of the water. A reservoir tank (25) was attached to the outlet of the cooling jacket to gather the hot water coming out from the condenser. Two water tanks were attached to the condenser throughout rubber tubes (19). The Lutron optical tachometer (28) was brought to measure the rotational speed of the engine. The experiment were set up to determine the thermal performance and thermal resistance of the thermosyphon using different organic working fluids at different filling ratios. The experiment was set to determine the results at different engine loads. The emissions and pollutants were spotted and monitored using the Ecom-D gas analyzer before and after the heat exchanger, as shown in Fig.3.



Figure 3(a). Probe intakes sample-before heat exchanger

Figure 3 (b) Probe intakes sample after heat exchanger.

The following procedures were followed consequently:

- The accelerator screw of the engine was adjusted to the position that gives a certain rpm of the engine, as a result, a certain amount of the exhaust gases and heat load. Three predetermined positions of the accelerator that gives three different speeds; 1400, 2100 and 2700 rpm. The three loads were defined using the optical tachometer. At the three preset speeds, the experiment took the same procedures all over again. The pressure difference in terms of cm of the manometer fluid was recorded; so as to determine the amount of the flue gasses passing through the duct.
- Then thermosyphon was charged with a certain predetermined amount of a chosen working fluid that needs to be investigated through the charging valve (29).
- Before starting up the engine, the cooling water was let to pass into the cooling jacket that is attached to the condenser section of the thermosyphon to avoid sudden pressure and temperature rise.
- The engine starts with a set predetermined speed.
- While the experiment reaches the steady state, a small amount of the vapor of the working fluid was discharged through the shut-off valve (22) to ensure that the pipe was free of noncondensable gases and air, this method was prechecked; as while turning off the engine for awhile and stop the experiment, the vacuum pressure gauges indicated that the internal pressure was about (-0.02 bar).
- After discharging a small amount of the working fluid in the vapor phase, the pressure decreases and temperature distrubtion along the tube changes; so additional time was given to reach the steady state again.
- The exhaust comes out from the engine was passing the exhaust duct in the certain path with the guidelines of the internally welded baffles to exchange heat with the evaporator section of the thermosyphon. The charged amount of the working fluid starts to change its phase from liquid to vapor. Each working fluid takes different times to reach the vapor phase; this is because of the different values of the latent heat of vaporization for each tested fluid. The amount of generated vapor was predetermined and calculated. Heat absorbed by the cooling water passing through the cooling jacket attached to the condenser section was predetermined at different mass flow rates of water.
- While the certain filling ratio of the chosen working fluid results were recorded, the engine was stopped and the thermosyphon was being washed using water and acetone and let to be dried before charging with next working fluid or changing another filling ratio.
- All readings were recorded at steady state, a little bit fluctuations, as a result of opening and closing of the exhaust valve of the engine, was overcome by recording the results in a timely manner, one minute trigging, and taking the average of the readings.

## III. DATA PROCESSING

Some formulas were used to determine the experiment limits, the maximum heat flux was determined using Rohsenow equation [6]:

$$\bar{\bar{q}}_s = \mu_L h_{fg} \left[ \frac{g(\rho_l - \rho_v)}{\sigma} \right]^{0.5} \left[ \frac{C_{p,l}\Delta T_e}{C_{s,f} h_{fg} P_{rl}^n} \right]^n \qquad (2)$$

While the minimum heat flux used formula is:

$$\bar{\bar{q}}_{min} = C h_{fg} \rho_v \left[ \frac{\sigma g(\rho_l - \rho_v)}{(\rho_l + \rho_v)^2} \right]^{0.25} \qquad (3)$$

The critical heat flux was deduced by:

$$\bar{\bar{q}}_{max} = C h_{fg} \rho \left[ \frac{\sigma g(\rho_l - \rho_v)}{\rho_v^2} \right]^{0.25} \qquad (4)$$

While the maximum generated vapor for the working fluid inside the thermosyphon is deduced by:

$$\dot{m}_{max} = \frac{\bar{\bar{q}}_{max} \pi D_i L_{ev}}{h_{fg}} \qquad (5)$$

The mass flow rate of the flue gasses is deduced using a deduced correlation from Bernoulli's equation [24]:

$$Q = C_f A_o \sqrt{\frac{2\Delta p}{\rho}} \qquad (6)$$

The absorbed heat at the condenser section is determined using this correlation:

$$Q_c = \dot{m} C_p \Delta T \qquad (7)$$

While the overall heat transfer coefficient of the thermosyphon is determined by:

$$U = \frac{Q_c}{\Delta T_m} \qquad (8)$$

$$T_m = T_{m,ev} - T_{m,co} \qquad (9)$$

The inaccuracy of measuring devices were shown in Table 1

TABLE.1.
INACCURACY OF MEASURING DEVICES

| Device | Inaccuracy |
|---|---|
| YOKOGOWA temperature recorder | ± 0.5 ℃ |
| Lutron optical tachometer | 0.05 % |
| Ecom-D gas analyzer | ±5% |
| K-type thermocouples | ± 1.5 ℃ |

The average uncertainty of the mass flow rate of cooling water, the heat absorbed in the condenser and the overall heat transfer coefficient are ±5.38 %, ±5.39 %, and ±7.62, respectively.

## IV. RESULTS AND DISCUSSIONS

The results of the experiemnet could be divided into two main groups: a) investigating the best working fluid among the others, b) investigating the selected working fluid in further procedures and parameters, besides, studying the influence of

cooling the exhaust flue gas temperature on carbon monoxide concentration.

### A. Organic Working Fluid Selection

In order to investigate the most proper working fluid among the others, we have maintained the engine speed constant at 1400rpm, and changed the filling ratios of each fluid with changing the mass flow rate of the cooling water to deduce the best thermal performance, besides, spotting the pollutants before and after the heat exchanger. This procedure was a potential indicator for the best organic working fluids that would be choosen for further experimental procedures. Thermophysical properties of the tested working fluids are shown in Table.2.

TABLE.2.
THERMOPHYSICAL PROPERITIES OF TESTED WORKING FLUIDS

| Fluid | Chemical Formula | Boiling Point [K |
|---|---|---|
| Benzene | $C_6H_6$ | 353.25 |
| Acetone | $C_3H_6O$ | 329.15 |
| Petroleum ether | $HC_3-O-CH_3$ | 363.15 |
| Chloroform | $CHCl_3$ | 343.35 |
| Water | $H_2O$ | 373.15 |

We prelimenary investigated each working fluid at FR=25% which is about 25 mL of the working fluid, the engine speed was maintened at 1400 rpm. The maximum temperature distribution occured when using chloroform as the working fluid, while the minimum distribution recorded by benzene and acetone, as shown in Fig.4. the best overall heat transfer coefficient also occured when using benzene as shown in Fig.5. which was about 140 $W/m^2.K$ at nearly 12 gm/sec of cooling water at the condenser
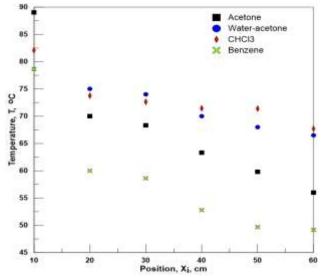


Figure. 4. Average temperature distribution along 25% filled thermosyphon for different working fluids at 1400 rpm.

Carbon monoxide concentration also played a vital role in selection process of the working fluid, the minimum concentration of carbon monoxide spotted was when using benzene, and no big differences were observed among the others, as shown in Fig.6. The recordings of pollutant

concentration was taken in timely manner by setting up the gas analyzer to print out the results each 3 minutes. The maximum observed was 3%. Another investigation was held also on these tested working fluids but with change of filling ratio, FR=50%, at the same engine speed. The benzene also overcome the other organic fluids, acetone came in the second place, while the chloroform and petroleum ether had bad responses in comparison to the benzene and acetone, as shown in Fig. 7.
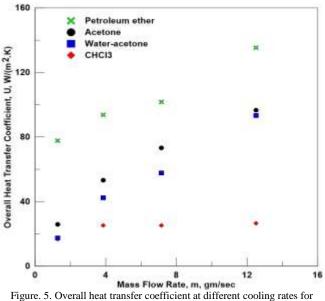


Figure. 5. Overall heat transfer coefficient at different cooling rates for FR=25% different working fluids at 1400rpm.
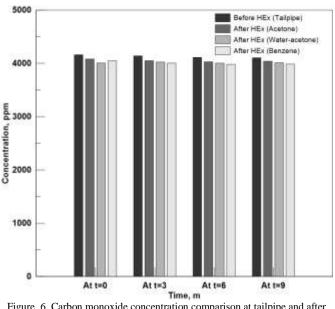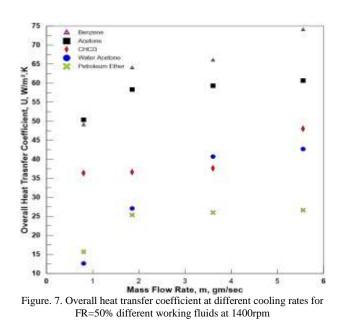


Figure. 6. Carbon monoxide concentration comparison at tailpipe and after heat exchanger charged with FR=25% of various working fluids at 1400 rpm

Benzene resulted in an overall heat transfer coefficient of 75 $W/m^2.K$ at 5.6 ml/sec coolant mass flow rate, as a result, benzene was selected due to its good thermal response, as the thermosyphon recorded the loweset thermal resistance to proceed further experimental investigations. By changing its

filling ratio, coolant mass flow rates and engine rotational speed to analyze its suitability in this application. Outlet and inlet temperature of the exhaust were recorded, as shown in Table.2, for each process to liaise the probability of an independency between the outlet temperature of the exhaust and gaseous carbon monoxide concentration.

TABLE.3. INLET

OUTLET TEMPERATURE AND CO REDUCTION PERCENTAGE OF THE EXHAUST AT 1400 RPM.

| Parameter | $T_{e,i}$ Inlet (℃) | $T_{e,o}$ outlet (℃) | Avg. CO Reduction % |
|---|---|---|---|
| No HEx | 89 | 89 | 0% |
| HEx - Acetone | 89 | 76 | 1.93% |
| HEx – Water acetone | 89 | 81 | 2.84% |
| HEx - Benzene | 89 | 68 | 3.01% |



Figure. 7. Overall heat transfer coefficient at different cooling rates for FR=50% different working fluids at 1400rpm

## B. Thermal Performance of Benzene Filled Thermosyphon

In order to investigate the overall thermal performance of the benzene filled thermosyphon in this heat recovery application, we have tested benzene in different working parameters. First of all, we charged the evaporator with benzene with FR=25% at different engine speeds 1400, 2100 and 2700 rpm and analyzing the temperature distribution along the tube, as shown in Fig.8, and its thermal resistance, as shown in Fig.9. Temperature distribution increased with increasing the engine speed. It was observed that at the middle speed, the minimum thermal resistance existed, as at the high engine speed, thermal resistance increased which would be a result of the burn out phenomena. The maximum overall heat transfer coefficient was 165 W/m$^2$.K at 5 ml/sec of cooling water and 2100 rpm. The maximum temperature difference of the cooling water was found to be 40.6$^0$C at 1 ml/sec. It was also deduced that while increasing the coolant mass flow rate, the amount of absorbed heat at the condenser increased, and temperature along the thermosyphon tube decreased. Which led to decreasing the thermal resistance and increasing thermosyphon's overall heat transfer coefficient. The temperature differences along the tube sections increases with

increasing the engine speed or the heat input parallel to increasing the mass flow rate of the coolant water. The maximum heat absorbed was about 310 W at 5 ml/sec and 2700 rpm. The thermal performance investigation for FR=50% of benzene was taken with the same sequence, the temperature distribution along the tube were recorded at engine speeds of 2100 and 2700 rpm respectively, as shown in Fig.10
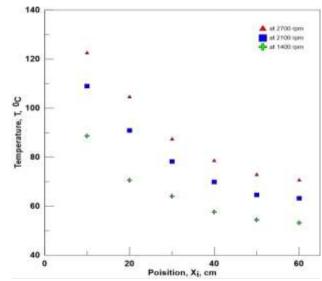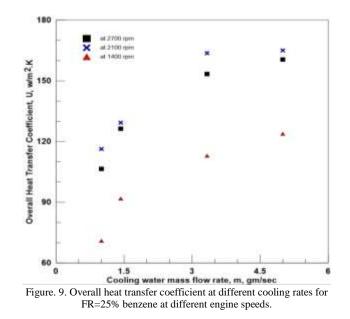


Figure. 8. Average temperature distribution along FR=25% benzene filled thermosyphon for at different engine speeds.



Figure. 9. Overall heat transfer coefficient at different cooling rates for FR=25% benzene at different engine speeds.

The highest temperature distribution was observed at 2700 rpm, the same as the previous investigation, as when increasing the engine speed, the amount of input heat increases, thereby, the temperature increases. The thermal resistance of the tube at 2700 rpm was less than that of 2100 rpm. The maximum heat transfer coefficient was about 222 W/m$^2$K at 5 ml/sec and 2700 rpm. The maximum temperature difference of the cooling water observed was 47.5$^0$C at 2100 rpm and 54$^0$C at 2700 rpm for 1 ml/sec flow rate. While the

maximum absorbed heat at the condenser was nearly 400 W at 5 ml/sec and running speed of 2700 rpm. It was observed that in FR=50%; temperautre differences across the tube sections were more than that of FR=25%, which led to a better thermal performance of the thermosyphon.
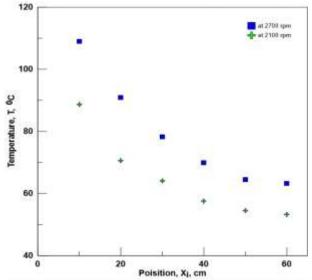
coolant flow rate. While the maximum water temperature difference existed was $34.5^0C$ at 1 ml/sec at 2700 rpm.



Figure. 10. Average temperature distribution along FR=50% benzene filled thermosyphon for at different engine speeds.



Figure. 12. Overall heat transfer coefficient at different cooling rates for FR=100% benzene at different engine speeds.



Figure. 11. Overall heat transfer coefficient at different cooling rates for FR=50% benzene at different engine speeds.
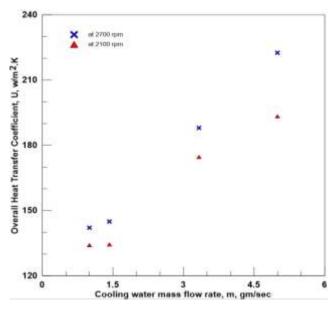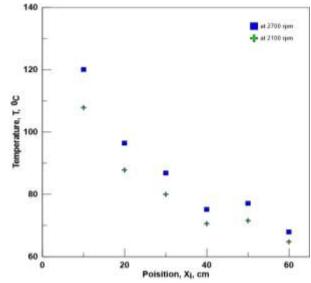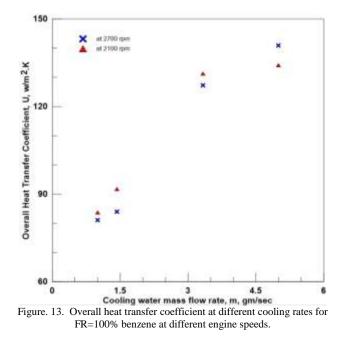


Figure. 13. Overall heat transfer coefficient at different cooling rates for FR=100% benzene at different engine speeds.

Another investigation was held by increasing the filling ratio to 100% at the three preset engine speed. Temperature distribution along the tube was higher at 2700 rpm than that of 2100 rpm, as shown in Fig.12, while the differences of the thermal resistance of the thermosyphon at both engine speeds was not significant, as shown in Fig.13. the maximum absorbed heat was about 140 W at 2700 rpm and 5 ml/sec of

Results of FR=50% of benzene was better than that of FR=25% & FR=100%, while the thermal performance of the tube with FR=25% comes in the second place and FR=100% was the worst. This agreed much with the literature reviews that used other fluids. The temperature distribtion of our case study is showed a logical sequence with comparing to Ashok [25] recordings while using methanol-ethanol mixture as working fluid at different heat inputs
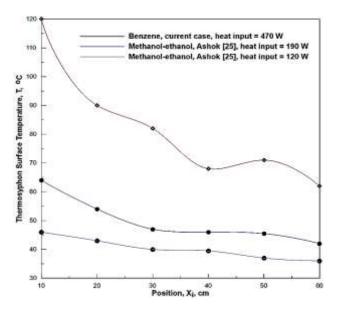
Figure. 14. Temperature distribution comparison between this case study and Ashok's experiment

## C.    Carbon Monoxide Reduction

In spotting carbon monoxide concentration, we've found that this heat recovery process has something to do with the reduction of its concentration. The optimum point which we measaured the concentration of the pollutants is while charging the thermosyphon with benzene at FR= 50%. Investigation was held on the three different speed of the engine. At 1400 rpm, the maximum carbon monoxide concentration before attaching the heat exchanger was 4161 ppm, while the minimum concentration was 4103 ppm in a 9 minute time frame. After attaching the heat exchanger, the maximum spotted concentration of (CO) was 3890 ppm, while the minimum concentration was 3694 ppm. A maximum reduction ratio of 10% of (CO) was recorded as shown in Fig.15.
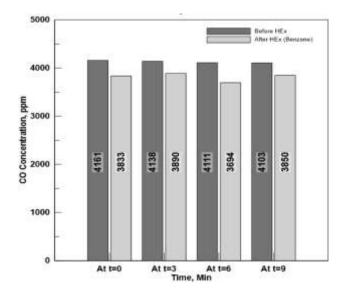
Comparing between CO concentration in the case of FR=25% of benzene, and the percentage in the case of FR=50$; it was obvious that the average percentage of concentration reduction has been increased by 4.49%. At 2100 rpm; carbon monoxide concentration was found to be reduced by a range of 275 to 402 ppm. The maximum recorded concentration of (CO) before attaching the heat exchanger was 3570 ppm, while the minimum recorded concentration was 3492 ppm in a 9 minutes time frame. After attaching the heat exchanger; it was found that the maximum concentration of (CO) was 3306 ppm, while the minimum concentration was 3090 ppm, as shown in Fig.16. A sensible reduction range of 7% to 12% was observed in the prementioned rotational speed. At 2700 rpm; maximum concentration of carbon monoxide before attaching the heat exchanger was 3294 ppm, while the minimum concentration was 3143 ppm. After attaching the heat exchanger, the maximum concentration was 2705 ppm, while the minimum concentration was 2568 ppm, as shown in Fig.17. A sensible reduction ratio of 14% to 22% was observed in this case.

The observation of pollutants reduction after cooling the flue gases confirms the conclusions of Ning, Cheung [19] research that upon cooling the flue gases, the mass concentration of the total particulate and the average diameter of the particulate increase, while the total particulate number decreases. The nucleation and condensation of the volatile organic materials has a vital role in this mechanism. But in our case, it's expected that coagulation was the main reason that confirmed this research hypothesis, as the Brownian motion [26] dominates the behavior of the particulate that exist in the exhaust, besides, the diffusion of the streamline of the flue gasses after exiting the tailpipe and the sudden restriction of the thermosyphon tube.



Figure. 16. Carbon monoxide concentration before and after attaching the heat exchanger at 2100 rpm, FR=50% benzene.



Figure. 15. Carbon monoxide concentration before and after attaching the heat exchanger at 1400 rpm, FR=50% benzene.
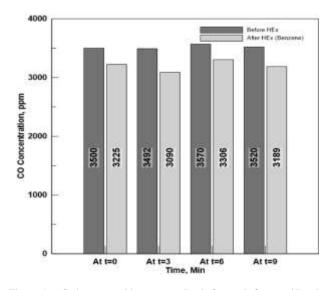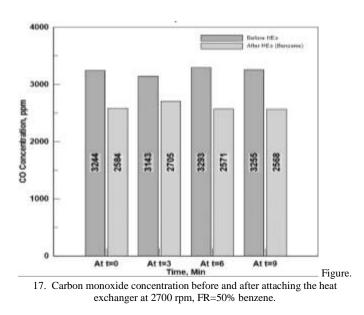
Figure. 17. Carbon monoxide concentration before and after attaching the heat exchanger at 2700 rpm, FR=50% benzene.

### V. CONCLUSION

This study presents an experimental investigation on thermal performance of two-phase closed thermosyphon, and its applicability in low temperature heat recovery solutions. Multiple organic working fluids, that are low in boiling point, were tested, then the best working fluid was selected to continue other investigations. The results can be concluded as the following:

- Benzene ($C_6H_6$) showed great thermal performance over other tested fluids, acetone comes in second place, while petroleum ether ($HC_3$-O-$CH_3$) resulted in worst thermal performance among the others, at different filling ratios FR= 25%, 50% and 100%.
- In organic thermosyphon; the optimum thermal performance was observed at FR=50%, this agreed much with the previous studies on other working fluids.
- Increasing in the coolant mass flow rate at the condenser section results in decreasing the temperature distribution along the thermosyphon, and increasing the absorbed heat from the condenser, which results in increasing the overall heat transfer coefficient of the thermosyphon.
- Increasing the engine load, increases the temperature distribution along the thermosyphon, increases the mass flow rate of the flue gasses, its temperature and heat input to the evaporator section..
- There is a sensible reduction of the carbon monoxide concentration after attaching the heat exchanger due to the heat exchanging process, which agreed with Ning, Z., et al experimental study.
- The highest reduction percentage of carbon monoxide was observed while charging the thermosyphon with benzene and recorded an average of 3.01% at FR=25% of different working fluids at 1400 rpm.
- CO reduction percentage increased with increasing the filling ratio of the benzene from 25% to 50% by 4.49% at the same rotational speed of 1400 rpm.

- The highest CO average reduction percentage observed was 19.33% at FR=50% bezene, while running the engine at 2700 rpm.

### REFERENCES

[1]. 1. Jordan Hanania, B.H., Kailyn Stenhouse, Jason Donev. *second law of thermodynamics, Waste Heat Statement*. 2012 [cited 2017; Available from: http://energyeducation.ca/encyclopedia/Second_law_of_thermodynamics#Waste_Heat_Statement.

[2]. 2. *Primary energy consumption worldwide from 1998 to 2016 (in million metric tons oil equivalent)*. 2017; Available from: https://www.statista.com/statistics/265598/consumption-of-primary-energy-worldwide/.

[3]. 3. Johnson, I. and W. Choate, *waste heat recovery, technology and oppotunities in US industry, 2008.* BCS, Incorporated, 2008.

[4]. 4. Ochterbeck, J.M., *Heat pipes.* Heat Transfer Handbook, 2003. **1**.

[5]. 5. Imura, H., et al., *Heat transfer in two-phase closed-type thermosyphons.* JSME Transactions, 1979. **45**: p. 712-722.

[6]. 6. Shiraishi, M., K. Kikuchi, and T. Yamanishi, *Investigation of heat transfer characteristics of a two-phase closed thermosyphon*, in *Advances in Heat Pipe Technology*. 1982, Elsevier. p. 95-104.

[7]. 7. Negishi, K. and T. Sawada, *Heat transfer performance of an inclined two-phase closed thermosyphon.* International Journal of Heat and Mass Transfer, 1983. **26**(8): p. 1207-1213.

[8]. 8. Terdtoon, P., S. Ritthidej, and M. Shiraishi. *Effect of aspect ratio and Bond number on heat transfer characteristics of an inclined two-phase closed thermosyphon at normal operating condition*. in *Proceedings of the 5* h International Heat Pipe Symposium*. 1996.

[9]. 9. Shalaby, M., et al., *Heat transfer performance of a two-phase closed thermosyphon.* Proceedings 6IHPS, Thailand, 2000: p. 269-278.

[10]. 10. Park, Y.J., H.K. Kang, and C.J. Kim, *Heat transfer characteristics of a two-phase closed thermosyphon to the fill charge ratio.* International Journal of Heat and Mass Transfer, 2002. **45**(23): p. 4655-4661.

[11]. 11. Ziapour, B.M. and H. Shaker, *Heat transfer characteristics of a two-phase closed thermosyphon using different working fluids.* Heat and mass transfer, 2010. **46**(3): p. 307-314.

[12]. 12. Naresh, Y. and C. Balaji, *Thermal performance of an internally finned two phase closed thermosyphon with refrigerant R134a: A combined experimental and numerical study.* International Journal of Thermal Sciences, 2018. **126**: p. 281-293.

[13]. 13. Wadowski, T., A. Akbarzadeh, and P. Johnson, *Hysteresis in thermosyphon-based heat exchangers and introduction of a novel triggering system for low-temperature difference heat-recovery applications.* Heat Recovery Systems and CHP, 1991. **11**(6): p. 523-531.

[14]. 14. Noie-Baghban, S.H. and G. Majideian, *Waste heat recovery using heat pipe heat exchanger (HPHE) for surgery rooms in hospitals.* Applied thermal engineering, 2000. **20**(14): p. 1271-1282.

[15]. 15. Arzbaecher, C., K. Parmenter, and E. Fouche. *Industrial waste-heat recovery: Benefits and recent advancements in technology and applications*. in *Proceedings of the ACEEE*. 2007.

[16]. 16. Chen, S. and J. Yang, *Loop thermosyphon performance study for solar cells cooling.* Energy Conversion and Management, 2016. **121**: p. 297-304.

[17]. 17. Orr, B., et al., *A review of car waste heat recovery systems utilising thermoelectric generators and heat pipes.* Applied Thermal Engineering, 2016. **101**: p. 490-495.

[18]. 18. Abu-Hamdeh, N.H., *Effect of cooling the recirculated exhaust gases on diesel engine emissions.* Energy Conversion and Management, 2003. **44**(19): p. 3113-3124.

[19]. 19. Ning, Z., C. Cheung, and S. Liu, *Experimental investigation of the effect of exhaust gas cooling on diesel particulate.* Journal of Aerosol Science, 2004. **35**(3): p. 333-345.

[20]. 20. Bauner, D., S. Laestadius, and N. Iida, *Evolving technological systems for diesel engine emission control: balancing GHG and local emissions.* Clean Technologies and Environmental Policy, 2009. **11**(3): p. 339-365.

[21]. 21. Prasad, R. and V.R. Bella, *A review on diesel soot emission, its effect and control.* Bulletin of Chemical Reaction Engineering & Catalysis, 2010. **5**(2): p. 69.

[22]. 22. Charalampos, A., K. Anastasios, and M. Stella, *The Effect of Temperature on Gas Emissions.* 2012.

[23]. 23. Reşitoğlu, İ.A., K. Altinişik, and A. Keskin, *The pollutant emissions from diesel-engine vehicles and exhaust aftertreatment systems.* Clean Technologies and Environmental Policy, 2015. **17**(1): p. 15-27.

[24]. 24. efunda. *Orifice Flow Meter Calculation.* 2018; Available from: http://www.efunda.com/formulae/fluids/calc_orifice_flowmeter.cfm.

[25]. 25. Ashok, M.F.N. and K. Mali, *Thermal Performance of Thermosyphon Heat Pipe Charged with Binary Mixture.* 2015.

[26]. 26. Hida, T., *Brownian motion*, in *Brownian Motion.* 1980, Springer. p. 44-113.